An *In Vivo* Human Time-Exposure Investigation of a Commercial Nano-Particle Solution

Mark A. Munger, Pharm.D.[*†], Przemyslaw Radwanski, Pharm.D., Ph.D.[‡], Greg Hadlock, Ph.D.[‡], Greg Stoddard, M.S.[†], Akram Shaaban, M.D.[¶], David Grainger, Ph.D.[§], and Garold Yost, Ph.D.[‡]

Departments of Pharmacotherapy*, Pharmacology and Toxicology‡, Pharmaceutics and Pharmaceutical Chemistry§, Internal Medicine†, and Radiology¶, University of Utah, Salt Lake City, Utah.

Corresponding Author

Mark A. Munger, Pharm.D.
University of Utah
30 South, 2000 East, Rm #201
Salt Lake City, Utah 84112-5820
Phone: (801) 581-6165
Fax: (801) 585-7316
mmunger@hsc.utah.edu

This study was funded in part by Award Number UL1RR025764 from the National Center for Research Resources.

Key Words: biological activity – nanoparticles
nanotechnology – nanotoxicology
safety research

Abstract

Background: Biodistribution, bioprocessing with possible toxicity of nanoscale silver is receiving increasing attention to human health.

Methods: We prospectively studied several time exposures of a commercial 10- and 32-ppm nanoscale silver solution in a double-blind, controlled, cross-over phase design. Healthy subjects (60) underwent complete metabolic, blood and platelet count, urinalysis, sputum induction, and chest and abdomen magnetic resonance imaging. Silver serum and urine content was determined.

Results: No clinically important changes in any metabolic, hematologic, or urinalysis measure identified were determined. No morphological (or structural) changes were detected in the lungs, heart (cardiac function) or abdominal organs. No significant changes were noted in pulmonary reactive oxygen species or pro-inflammatory cytokine generation.

Conclusion: *In vivo* oral exposure of a commercial nanoscale silver solution does not exhibit clinically important changes in metabolic, hematologic, urine, vital sign changes, physical findings or imaging changes visualized by MRI. Further study of increasing time-exposure, dose, and additional organ systems is warranted.

Introduction

The age of nanotechnology is driving potentially the most important engineering revolution since the industrial age. There are over 1,300 manufactured nanotechnology enabled consumer products in the marketplace today.[1] This revolution has afforded silver a reemergence as a medical modality.[2-4] Nanoscale silver makes up approximately a quarter of the inventory of commercially available nanoproducts. Silver exhibits physiochemical attributes and biological activity broadening its application as an antibacterial, anti-viral, and anti-inflammatory therapy.[4-9] With greater systemic applications to the human condition, penetration of silver nanoparticles across cell membranes could result in vascular redistribution presenting the potential for evasion of immune cellular clearance, leading to systemic acute or chronic cytotoxicity or illness.[4]

A growing body of in vitro evidence supports that silver nanoparticles, in concentrations primarily between 5-50 µg/ml, may be toxic to mammalian cells. A variety of tissues including the lung,[10-13] liver,[11,14-17] brain,[18] vascular system[19] and reproductive systems[20-21] may be negatively influenced. The lung and liver may be the most targeted with prolonged exposure.[10, 13] Given the trajectory of new nanoscale products, especially silver-based, being introduced into the consumer marketplace it is important to understand whether these in vitro findings translate to human toxicity.[22]

To this end, we studied 60 healthy volunteers through several time-length exposures in a prospective, randomized, placebo-controlled, single-blind, dose-monitored, cross-over design to quantitate changes in metabolic, hemotologic, and suptum morphology and to qualitate changes in physical findings and organ imaging from a commercially available silver nanoparticle 10 and 32 ppm solution.

Methods

Study Population

The two studies were conducted at the University of Utah Lung Health Study Clinic and Center for Clinical and Translational Sciences at University Hospital. Each prospective subject underwent a screening evaluation to assess eligibility for enrollment. Sixty healthy volunteers were subsequently enrolled in two separate studies (i.e., 10 ppm [36 subjects] and 32 ppm [24 subjects], respectively) between 18-80 years of age. Subjects were excluded with a history of any heavy metal allergy; asthma, chronic bronchitis or emphysema; or renal impairment defined by a creatinine clearance ≤ 30 ml/minute; or significant acute or chronic disease as determined by the investigators. Females of child-bearing potential, defined as women physically capable of becoming pregnant, including women whose career, lifestyle, or sexual orientation precludes intercourse with a male partner and women whose partners are using 2 barrier birth control methods or hormonal contraceptive method. Any female subject who was nursing was excluded. Subjects who were unable to complete the study were excluded from analysis.

All patients were provided written informed consent before participating in any study procedures. The study was conducted in accordance with the International Conference on Harmonisation of Technical Requirements for Registration of Pharmaceuticals for Human Use Guidelines for Good Clinical Practice

and the Declaration of Helsinki, and received approval from the University of Utah Institutional Review Board. The trials are registered with Clinical-Trials.gov (Identifier: NCT01243320 and NCT01405794).

Both studies were overseen by an independent Data Safety and Monitoring Board which reviewed each individual subject's and the study population data in aggregate, granting approval of safety from the lesser time-period before the study was allowed to proceed to the next period.

Study Product

The study product was manufactured by American Biotech Laboratory (Alpine, Utah) as a reduced elemental silver colloidal dispersion in water (USP 7,135,1095). The silver is in the form of zero-valent elemental silver coated with silver oxide (Ag_4O_4). The reduced silver ions have a particle size average between 5-10 nm (10 ppm) or 25-40 nm (32 ppm), respectively. The average daily ingestion of elemental silver used in this study is estimated to be 100 mcg/day for 10 ppm and 480 mcg/day for 32 ppm.

Study Design for Metabolic, Silver Concentrations, Induced Sputum, and MRI

Each subject initially received the silver nanoparticle solution diluent (e.g. sterile water [no silver nanoparticles]) followed by the active silver nanoparticle solution for a period of 3-, 7- and 14-day periods, respectively. The 10 ppm solution was provided in 3-, 7-, and 14-day time periods, the 32 ppm for a 14-day period only. There was a 72-hour washout period prior to study drug cross-over. Each subject received 15 millileters of study medication daily from a pre-mixed oral syringe. Each dose was observed daily by study personnel to ensure compliance. Subjects were blinded to the study product received.

At baseline and the end of each time-period, subjects underwent a medical and drug history, a complete physical examination, comprehensive metabolic panel, blood count with differential and complete urinalysis. Blood and urine were collected for serum and urine silver concentrations at trough concentrations (≥24 hours post-dose) for the 3- and 7-day time periods at 10 ppm and at peak concentration (≤ 2 hours post-dose) for the 14-day 10 ppm dose and for the 32 ppm study population. Silver serum or urine concentrations were determined by Inductively Coupled Mass Spectrometry (NMS Laboratories, Willow Grove, Pennsylvania). Calibration samples are in dilute nitric acid and controls are in human serum. The quantization limit of the samples for this study were 0-40 mcg/L. Silver concentrations were determined at either trough (24 hours post-dose) or at peak (≤2 hours post-dose).

Sputum was collected by induction protocol within 24 hours of the last dose of each time-period, as previously described.[21] Briefly, subjects inhaled increasing concentrations of nebulized hypertonic saline of 3-10% solution from Devilbiss Pulmo Aide Compressor (Specialty Medical Supply, Milford, Ohio) fitted with Sidstream High Efficiency Nebulizer (Cardinal Health, Dublin, Ohio) without valve or nose clips. Sputum induction time between 15-30 minutes was used for all subjects. The protocol was stopped at 30 minutes, if the FEV_1 dropped by ≥20%, or whenever a quality sample was obtained.

Sputum Analysis:

Determination of hydrogen peroxide production.

Hydrogen peroxide concentrations were determined using a modification of the method described by Cameron et al. (1999). Briefly, after cells were removed from the sputum samples (described previously), 5 units of horseradish peroxidase (HRP) were added to the samples, and then the total sample volumes were brought to a final volume of 1.0 mL with 1mM 2,2-azino-bis(3-ethylbenzthiazoline-6-sulfonic acid) (ABTS). After incubating for 20 min at room temperature, samples were filtered using a Kimwipe to remove mucus and other debris and ABTS radical formation was quantified spectrophotometrically at 650 nm.

Measurement of peroxiredoxin (Prx) protein expression.

Cells collected from the induced sputum samples were pelleted, resuspended in TRIzol (Invitrogen, Carlsbad, CA) and GlycoBlue (Invitrogen), and frozen at -80 °C until processing. After all patient samples were collected, RNA and protein was isolated using TRIzol according to the manufacturer's instructions. The isolated protein was resuspended in 1% sodium dodecyl sulfate and 4 M urea and heated for 1 h at 50 °C. The isolated RNA was retained for quantitative PCR (described below). Protein concentrations were determined using the Bicinchoninic Acid assay kit (Pierce, Rockford, IL). Equal quantities of total protein (~50μg) were electrophoresed through a 12% NuPAGE gel (Invitrogen) and subsequently transferred to a polyvinylidene difluoride membrane. The membranes were blocked using 5% (w/v) dry milk for 24 h at 4°C. The membrane was then incubated with a polyclonal rabbit anti-$PrxSO_3$ antibody (ab16830; Abcam, Cambridge, MA), which recognizes both the sulfinic and sulfonic forms of Prx, diluted in 2.5% (w/v) dry milk (1: 2000) overnight at 4°C. The membranes were then washed 2 times in phosphate buffered saline with Tween (PBST) and incubated with a goat anti-rabbit HRP conjugated secondary antibody (ab6721; Abcam) diluted in 2.5% (w/v) dry milk (1: 2000) for 1 h at room temperature. After washing 3 times in PBST, the bands were visualized using the Pierce ECL plus chemiluminescent Western blotting substrate (ThermoScientific, Waltham, MA) on a Kodak image station 440 (Kodak, Rochester, NY). Relative band intesitities were quantified using the Kodak 1D image analysis software (Kodak).

Determination of RNA expression using quantitative real-time PCR (qPCR).

Total RNA was extracted as described above. Total RNA (0.5 μg) was converted to cDNA using Superscript III (Invitrogen). The resultant cDNA was diluted 1: 50 in RNase-free ddH_2O for analysis by qPCR using the LightCycler 480 SYBR Green I Master Mix (Rocher, Indianapolis, IN) on a LightCycler 480 system (Roche) using the LightCycler 480 software (Roche). The PCR program consisted of a10 min incubation at 95 °C, followed by 40 cycles of 95 °C for 15 s, 55 °C for 30 s, and 72 °C for 30 s. Experiments were performed in triplicate and standardized to the β2 macrogobulin (β2M) gene. Primer sequences were (5' → 3'): h β2M sense-GATGAGTATGCCTGCCGTGTG and antisense-CAATCCAAATGCGGCATCT; hIL-1α sense-CGCCAATGACTCAGAGGAAGA and antisense-AGGGCGTCATTCAGGATGAA; IL-1β sense-CTGTCCTGCGTGTTGAAAGA and antisense-TTGGGTAATTTTTGGATCTACA; hIL-8 sense-ACTGAGAGTGATTGAGAGTGGAC and antisense-AACCCTCTGCACCCACTTTTC; hMCP1 sense-TTCTGTGCCTGCTGCTCAT and antisense-GGGGCATTGATTGCATCT; hNQ01 sense primer: ATGTATGACAAAGGACCCTTCC hNQ01 anti-sense primer: TCCCTTGCAGAGAGTACATGG hCRP sense-CTTGACCAGCCTCTCTCATGC and antisense-CGTGTAGAAGTGGAGGCACA; hiNOS sense-GTCACCTATCGCACCCGAGATG and antisense-GCCACTGACACTCCGCACAAAG; and hIL-6 sense-AACCTGAACCTTCCAAAGATGG and antisense-TCTGGCTTGTTCCTCACTACT.

MRI Protocols

A cardiac and abdominal MRI were obtained at the end of each phase of each time-period. Patients were examined on a 1.5-T, 32-channel superconducting MR system (Magnetom Avanto, Siemens Medical Solutions) with high-performance gradients (maximum gradient strength, 45 mTm^{-1}; maximum slew rate, 200 $mTm^{-1}s^{-1}$).

Cardiac MRI studies were carried out using breath-hold acquisitions prospectively triggered by the ECG. The imaging protocol included multiplanar fast imaging with steady-state precession (SSFP) and delayed enhancement imaging.

Cine SSFP (TrueFISP) images were acquired in multiple standard short-axis and long-axis views, including specific RVOT and LVOT orientations, using; slice thickness 8 mm, echo time 1.2 ms, pixel bandwidth 1.150 Hz, repetition time 3.0 ms, temporal resolution about 43 ms, matrix 256 × 202). The field of view was 340 mm on average and adapted to the size of the patient, leading to a spatial resolution of about 2.4 × 1.4 × 8 mm. Abdominal MRI protocol included a transverse T1-weighted fast gradient-recalled dual-echo sequence (TR/in-phase TE/out-of-phase TE, 129/4.36/2.0; flip angle, 70°; matrix, 134 x 256; section thickness and intersection gap, 6 and 0.6 mm; signal average, 1; field of view, field of view, 220–340 mm [depending on body habitus])) and a transverse T2-weighted HASTE (TR/TE, 1,000/89; refocusing angle, 180°; slices, 20; slice thickness, 6 mm with a 10% gap; matrix, 168–192 × 256; field of view, 220–340 mm [depending on body habitus]).

A dynamic contrast-enhanced 3D gradient-echo volumetric interpolated breath-hold examination (VIBE) sequence was performed in the arterial, venous, and delayed, after the injection of 0.1 mmol/kg of body weight of Gadopentetate dimeglumine (Magnevist; Bayer HealthCare Pharmaceuticals, Berlin, Germany) at rate of 2 mL/s using a pressure injector. This was followed by delayed contrast-enhanced cardiac study using a segmented inversion–recovery sequence in the same views used for cine cardiac MRI 10–20 min after contrast administration.

All images were deidentified and transferred to a 3D postprocessing workstation (Leonardo, Siemens Healthcare). LV function and volumes were calculated by planimetry of the endocardial and epicardial borders from the serial short-axis views (usually 8–14) with no gap between the slices. Ejection fraction, end diastolic volume and end systolic volume were analyzed.

Statistical Analysis

The power of the study to detect toxicity was determined by the hypothesis that there would be no toxicity observed at any time-period. There were a total of 36 subjects in the 3-, 7-, and 14-day periods at 10 ppm and 24 subjects at the 14-day period for 32 ppm in a crossover design. This enrollment provides an 80% probability, of indentifying a toxicity problem, if toxicity is as common as 6.5%, based on a binomial probability and using 1-Prob (observed incidence=0|true incidence=0.065). Combining the 10 ppm and 32 ppm solutions, for a total sample size of n=60, based on a binonimal probability, there was an 80% probability of observing toxicity in at least one study subject if the true toxicity incidence is 2.7%. For the analysis examining paired sample mean differences between placebo and active solution, the n=24 subjects with maximum exposure, 32 ppm for 14 days, provided 80% power to detect a mean difference of 0.48 standard deviations (SD), using a two-sided alpha 0.05 comparison and assuming a correlation of r=0.70 between the placebo and active phases. For the total sample of n=60, there was 80% power to

detect a 0.30 SD difference. Assuming the placebo phase is centered in the normal laboratory reference range, with 2 standard deviations in either direction for the mean of the active solution phase to go outside of the normal reference range, or a 2 SD difference, the effect sizes of 0.48SD and 0.30SD represented detectable effects well within any given normal laboratory reference range.

The analysis used two approaches for the data analysis: 1). A mixed effects linear regression with measurements nested within each subject used to examine an average effect, and 2). Individual observations examined descriptively with standard reference ranges (±2 standard deviations[SD]) and extended reference ranges (±4 SD) to access toxicity in individual subjects. To account for skewness and outliers, analogous intervals with equivalent inclusion probabilities were formed from the median and appropriate multiples of the interquartile range. The primary analysis of clinical toxicity was determined if in any subject, from any of the three exposure time-periods, and for each of the outcomes measured, by any value that changes by 2 times the upper limit of normal (ULN), as defined by the normal range from Associated Regional University Pathologists Laboratory, (ARUP) Salt Lake City, Utah of the mean baseline value of the subjects. The clinically significant toxicity bound was set at twice the ARUP ULN or mean+4SDs. If a subject crossed this bound during either phase of the time-period, it was concluded that the subject experienced a toxicity event. Any MRI event will be qualitatively described.

Results

A total of 62 subjects were enrolled in the study. Sixty subjects completed the study. Two were discontinued due to inability to draw blood (subject never received study product) and hospitalization for pulmonary embolism (subject only received 12 days of placebo-diluent), respectively. The population is described in Table 1.

Changes in Body Mass Index (BMI), Blood Pressure and Heart Rate

Changes in subject hemodynamics are listed in Table 2. No clinically important changes in weight, BMI, systolic or diastolic blood pressure or heart rate were noted. However, heart rate significantly declined by 2.3 beats per minute for the total group, but not for the individual dosing groups.

Comprehensive Metabolic Panel, Complete Blood Count with Differential and Urinalysis Findings

Results of the complete metabolic panel are listed in Table 3. There were no statistically significant or clinically important changes in any laboratory finding through in the total population studies, independent of time-period exposure. Blood urea nitrogen and alanine aminotransferase tests from the 10 ppm dose were statistically significant, but nothing in the 32 ppm dose were noted. However, when the 95% CI limits of these significant tests are added to the mean value of the active period, representing a statistical comparison to the normal reference range limits, all values remain within these limits, without statistical important inference. To further understand whether toxicity may be related to exposure time, we conducted a mixed effects linear regression analysis while controlling for the baseline value for all 36 subjects in the 10 ppm. There was no statistical significance in any comprehensive metabolic panel test, suggesting increasing exposure time does not increase toxicity response at the 10 or 32 ppm dose. Chronological age or gender was not associated with any change in any clinical metabolic test.

The results of the complete blood count with differential are displayed in Figure #1. Comparison of the red blood cell count (RBC) between active vs. placebo solutions was statistically significant in the 10 ppm dose, without significance in the 32 ppm or the total sample analysis. When the linear regression model was applied to the comparison, there was no significance. There were no clinically important changes in any blood count value including erythrocytes, granulocytes, or agranulocyte counts. Exposure time did not show significance with any blood count value, nor was age or gender a determinate of change.

There were no statistically significant or clinically important changes in the complete urinalysis, including continuous variables of urine specific gravity, pH, or urine urobilogen. Although there were individual subject positive tests for urine ions, proteins, blood cells, and some other molecules, these changes remained unchanged in comparison between the active and placebo solutions at 10 ppm, 32 ppm or in the total sample.

Serum Silver and Urine Concentration Findings

Serum silver and urine silver concentrations were determined at different time variables related to the time of dose. There was no detection of serum silver from any subject at trough concentrations throughout the 3- and 7-day time periods of 10 ppm. Peak serum silver concentration was detected in 42% of subjects in the 14-day 10 ppm showing a mean of 1.6±0.4 mcg/L. The 32 ppm dose mean concentration was detected in 92% of subjects at 6.8±4.5 mcg/L. Four 32 ppm subjects showed concentrations ≥ than the lower limit of quantitation for toxic concentrations as determined by NMR Laboratory (range: 11-40 mcg/L). No detection of silver was determined in the urine, independent of dose or time period.

Sputum Reactive Oxygen Species and Pro-Inflammatory Cytokine RNA Findings

Quality paired samples allowing determination of reactive oxygen species concentrations and pro-inflammatory cytokine RNA expression from induced sputum samples were analyzed in 72% and 83% of 10 ppm and 32 ppm study population, respectively (Table 4). There was no statistically significant change in hydrogen peroxide production or Prx expression based on dose, study population or time period. Analysis of IL-8, IL-1α, IL-1β, MCP1 and NQO1 also showed no statistical difference between the active silver and placebo solutions at either dose, total study population, or based on time frame.

MRI Findings

Eighteen 10 ppm and eleven 32 ppm subjects underwent a post 3-14 day, respective active and placebo solution cardiac and abdominal MRIs. No morphological or structural changes were noted with active compared to placebo in any subject. There was no detection of silver coalescence or aggregation on any MRI image.

Discussion

Nanoscale silver has the widest degree in integration of commercialization including consumer products, medical devices, and pharmaceuticals.[1] Therefore, the study of this nanoscale source is critically

important to our understanding of potential human toxicity of this field. Sources of nanoscale silver include, but are not limited to, the textile, food, cosmetic, biosensor and electronic industries. Furthermore, the potential for use of silver nanoparticles in the disease detection and treatment may lead to increased exposure to the human state. To determine the human risk of a commercial nanoscale silver product we conducted a prospective, controlled, parallel design systematic *in vivo* study of two doses of a commercial silver nano-particle solution over a 3-14 day monitored exposure. Our findings show that this product is distributed into human serum but does not demonstrate clinically significant changes in metabolic, hematologic, urine, vital sign changes, physical findings, sputum morphology or imaging changes as visualized by MRI. To our knowledge, this is the first systematic *in vivo* study of any systemic nanoscale product.

Many authors have detailed the potential for human toxicity from nano-particles. Suggested and defined target organ systems which may result from nano-particle adverse health effects include the pulmonary, cardiovascular, neurologic, reticuloendotheilal, renal, or reproductive systems.[23-26] To this end, the literature has called for a new toxicological science to establish procedures to test the use of nanoparticles in the marketplace, as well as the critical need for *in vivo* studies.[27-28] Our study starts to answer existent human toxicity in a systematic way.

Abdominal organ system toxicity has been shown to occur from exposure to silver nanoparticles. The liver, in particular, has been noted as a toxicity target, possibly due to oxidative stress.[13] Non-cytotoxic doses of silver nanoparticles reduced mitochondrial function, cell profileration, and induced apoptosis in rat and human liver, and human mesenchymal cell lines, respectively.[13-14, 29] We have shown in MDR1.C and Hep G2 cell lines that after 24 hour exposure of a commercial 32 ppm silver nanoparticle solution, where cell viability was maintained, that nanoscale silver maybe a potential source of drug-drug interactions.[30] Potential interactions may occur through reductions in NADPH cytochrome c reductase activity (citation?). In contrast, a prospective, controlled 90 day exposure of 56 nm silver nanoparticles at 30 mg/kg *in vivo* rat study did not show any clinical chemistry, hematological, body weight, food consumption, or water intake changes.[31] Our human clinical findings correlate closely with these results. Hence, potential *in vitro* hepatocellular toxicity could occur from non-cytotoxic doses of nanoscale silver but these results do not correlate with *in vivo* rat or our human findings. Reasons for this disconnect may be *in vitro* direct cell exposure time or incomplete understanding of *in vivo* bioavailability, distribution, or liver blood flow dynamics of the nanoscale silver. MRI results from this study were not able to differential any abdominal changes from exposure to nanoscale silver.

The lung is another major target of silver nanoparticle exposure, particularly through inhalation. Silver nanoparticles (15-18 nm) may bind to lung epithelial cells and alveolar macrophages, producing reactive oxygen species, potentially limiting function of cells.[9-10, 12, 32] Histopathological examination from inhaled 18 nm silver nanoparticles for 90 days in Sprague-Dawley rats show dose-dependent alveolar infiltration, thickened alveolar walls and small granulomatous lesions.[12] These histology changes were associated with reductions in tidal and minute volumes. Congruence of results from multiple *in vitro* and a single *in vivo* animal model support cellular and functional toxicity from inhaled nanoscale silver. However, oral dosed nanoscale silver from our study failed to induce changes in reactive oxygen species or pro-inflammatory cytokine RNA from induced sputum samples. This probably is due to a lack of translocation of these particles to the respiratory system from the gastrointestinal route.

Further studies are necessary to understand the potential of nanoscale silver toxicity on the human reproductive system, systemic toxicity from subcutaneous delivery systems or from leaching of imbedded silver in catheter-based medical equipment, and to the central nervous system from multiple delivery systems. We did not specifically study these other physiologic systems or other delivery systems. Our study time frame of 14 days, although a moderate time, needs to be extended in order to determine whether longer exposure leads to accumulation of nanoscale silver in human lipid compartments, which may result in chronic toxicity.

In summary, nanoscale silver is an important biomaterial in the current engineering nano-revolution. We have demonstrated that monitored dosing over a 14-day period of a commercially available oral nano-silver product does not realize in clinically important toxicity across a wide variety of physiological parameters. Further study of longer durations is clearly warranted.

Acknowledgement: The authors express their appreciation to Cassandra Rice, Ph.D., G. Martin Villegas, M.S. and the staff of the Utah Lung Health Study Clinic, Kimberly Morley, M.D., Aaron Luebke, M.D., Melissa Reily, M.D., Karla Miller, M.D., for their technical and clinical support.

References

1. The Project on Emerging Nanotechnologies. Nanotech-enabled Consumer Products Continue to Rise. http://www.nanotechproject.org/news/archive/9231/

2. Alt V, Bechert t, Steinrucke P, Wagnener M, Seidel P, Dingeldein E. et al. An *in vitro* assessment of the antibacterial properties and cytotoxicity of nanoparticle silver bone cement. Biomaterials 2004;25:4383-91.

3. Moiemen NS, Shale E, Dryadale KJ, Smith G, Wilson TT, Papini R. Acticoat dressing and major burns: Systemic silver absorption. Burns 2011;37:27-35.

4. Vaidyanathan R, Kalishwaralal K, Gopalram S, Guranathan S. Nanosilver—The burgeoning therapeutic molecule and its green synthesis. Biotechnol Adv 2009;27:924-37.

5. Samberg ME, Orndorff PE, Monteiro-Riviere. Antibacterial efficacy of silver nanoparticles of different sizes, surface conditions and synthesis methods. Nanotoxicol 2011;5(2):244-53.

6. Roy R, Hoover MR, Bhalla AS, et al. Ultradilute Ag-aquasols with extraordinary bacteriocidal properties: Role of the system Ag-0-H_20. Mat Resear Innovat 2007;11:3-18.

7. Atiyeh BS, Costagliola M, Hayek SN, Dibbo SA. Effect of silver on burn wound infection control and healing; review of the literature. Burns 2007;33:139-48.

8. Elechiguerra JL, Burt J, Morones JR, Camacho-Bragado A, Gao X, Lara HH, Yacaman MJ. Interaction of silver nanoparticles with HIV-1. J Nanobiotechnol 2005;3:6

9. Bhol KC, Alroy J, Schechter PJ. Anti-inflammatory effects of topical nanocrystalline silver cream on allergic contact dermatitis in a guinea pig model. Clin Exp Dermatol 2004;29:282-7.

10. Takenaka S, Karg E, Roth C, Schultz H, Ziesenis A, Heinzmann U, Schramel P, Heyder J. Pulmonary and systemic distribution of inhaled ultrafine silver particles in rats. Environ Health Perspect 2001;109:(Suppl 4)547-51.

11. Carlson C, Hussain SM, Schrand AM, Braydich-Stolle LK, Hess KL, Jones RL, Schlager JJ. Unique cellular interaction of silver nanoparticles: size-dependent generation of reactive oxygen species. J Phys Chem B 2008;112(43):13608-19.

12. Soto K, Garza KM. Murr LE. Cytotoxic effects of aggregated nanomaterials. Acta Biomater 2007;3:351-8.

13. Sung JH, Ji JH, Yun JU, et al. Lung function changes in Sprague-Dawley rats after prolonged inhalation exposure to silver nanoparticles. Inhal Toxicol 2008;20(6):567-74.

14. Hussain SM, Hess KL, Gear hart JM, Geiss KT, Schlarger JJ. In vitro toxicity of nanoparticles in BRL 3A rat liver cells. Toxicol in Vitro 2005;19:975-83.

15. Arora S, Jain J, Rajwade JM, Paknikar KM. Interactions of silver nanoparticles with primary mouse fibroblasts and liver cells. Toxicol Appl Pharmacol 2009;236:310-8.

16. Park EJ, Yi J, Kim Y, Choi K, Park K. Silver nanoparticles induce cytoxicity by a Trojan-horse type mechanism. Toxicol in Vitro 2010;24:872-8.

17. Kawata K, Osawa M, Okabe S. In vitro toxicity of silver nanoparticles at noncytotoxic doses in HepG2 human hepatoma cells. Environ Sci Technol 2009;43:6046-51.

18. Hussain SM, Javorina AK, Schrand AM, Duhart HM, Ali SF, Schlager JJ. The interaction of manganese nanoparticles with PC-12 cells induces dopamine depletion. Toxicol Sci 2006;92(2):456-63.

19. Rosas-Hernandeza H, Jimenez-Badilloa S, Martinez-Cuevasa PP, et al. Effects of 45-nm silver nanoparticles on coronary endothelial cells and isolated rat aortic rings. Toxicol Lett 2009;191(2-3):305-13.

20. Braydich-Stolle L, Hussain S, Schlager JJ, Hofmann MC. In vitro cytotoxicity of nanoparticles in mammalian germline stem cells. Toxicol Sci 2005;88:412-9.

21. Ahamed M, Karns M, Goodson M, Rowe J, Hussain SM, Schlager JJ, Hong Y. DNA damage response to different surface chemistry of silver nanoparticles in mammalian cells. Toxicol Appl Pharmacol 2008;233(3):404-10.

22. Gibson PG, Wlodarczyk JW, Hensley MJ, Gleeson M, Henley RL, Cripps AW, Clancy RL. Epidemiological association of airway inflammation with asthma symptoms and airway hyperresponiveness in childhood. Am J Respir Crit Care Med 1998;158;356-41.

23. Gwinn MR, Vallyathan V. Nanoparticles: Health Effects—Pros and Cons. Environ Health Prospect 2006;114:1818-25.

24. Panyala NR, Peña-Mèndez EM, Havel J. Silver or silver nanoparticles: a hazardous threat to the environment and human health? J Appl Biomed. 2008;6:117-129.

25. Xia T, Li N, Nel AE. Potential health impact of nanoparticles. Annu Rev Public Health 2009;30:137-50.

26. Ahamed M, Alsalhi MS, Siddiqui MKJ. Silver nanoparticle applications and human health. Clinica Chimica Acta 2010;411:1841-8.

27. Nel A, Xia T, Mädler L, Li N. Toxic Potential of Materials at the Nanolevel. Science 2006;311:622-7.

28. Fischer HC, Chan WCW. Nanotoxicity: the growing need for an *in vivo* study. Curr Opin Biotech 2007;18:565-71.

29. Greulich C, Kittler S, Epple M, Muhr G, Koller M. Studies on the biocompatibility and the interaction of silver nanoparticles with human mesenchymal stem cells (hMSCs). Langerbecks Arch Surg 2009;394:495-502.

30. Lamb JG, Hathaway, Munger MA, Raucy JL, Franklin MR. Nanosilver particle effects on drug metabolism in vitro. Drug Metab Dispos 2010;38:2246-51.

31. Kim YS, Song MY, Park JD, Song KS, Ryu HR, Chung YH, Chang HK, Lee JH, Oh KH, Kelman BJ, Yu IJ. Subchronic oral toxicity of silver nanoparticles. Part Fibre Toxicol 2010;20.

32. Xia T, Kovochich M, Brant J, Hotze M, Sempf J, Oberley T, Sioutas C, Yeh JI, Wiesner MR, Nel AE. Comparison of the abilities of ambient and manufactured nanoparticles to induce cellular toxicity according to an oxidative stress paradigm. Nano Lett 2006;8:1795-1807.

Tables

Table 1: Study Population Demographics

Demographic/Clinical Variable	10 ppm (n=36)	32 ppm (n=24)	Total Sample (n=60)
Age, years Range	52±11 26-76	41±15 20-67	47±14 20-76
Gender, n M/F (%)	17/19 (47/53)	18/6 (75/25)	35/25 (58/42)
BMI (kg/m^2) mean±SD (max-min)	29±6 20-45	29±6 21-43	29±6 20-45
SBP (mmHg) mean±SD (max-min)	127±19 176-84	127±13 150-102	127±17 176-84
DBP (mmHg) mean±SD (max-min)	83±11 106-55	81±11 107-62	82±11 107-55
Heart Rate (bpm) mean±SD (max-min)	69±9 84-42	65±7 79-52	68±8 84-42

Table 2: Study Population Changes in Hemodynamics

Hemodynamic Variable	10 ppm Mean Change [95% CI: min, max] (*p* value)	32 ppm Mean Change [95% CI: min, max] (*p* value)	Total Sample Mean Change [95% CI: min, max] (*p* value)
Weight (kg)	-1.1[-2.6, 0.4] (0.17)	-0.2[-0.1, 0.8] (0.14)	-0.5[-1.4, 0.4] (0.30)
BMI (kg/m^2)	-0.4[-0.9, 0.1] (0.15)	-0.1[-0.04, 0.3] (0.14)	-0.2 [-0.5, 0.1] (0.26)
SBP (mmHg)	1.3[-1.7, 4.3] (0.40)	-1.3[-3.0, 5.6] (0.54)	1.3[-1.2, 3.8] (0.30)
DBP (mmHg)	-2.4[-5.5, 0.7] (0.13)	-0.7[-2.5, 3.8] (0.67)	-1.2 [-3.4, 1.1] (0.31)
HR (bpm)	-1.9[-5.0, 1.3] (0.25)	-1.2[-6.0, 3.5] (0.61)	-2.3 [-4.6, -0.93] (0.05)

BMI: Body Mass Index; SBP: Systolic blood pressure; DBP: Diastolic Blood Pressure; HR: Heart Rate

Table 3: Study Population Comprehensive Metabolic Panel (10 ppm [n=36], 32 ppm [n=24], Total Sample [n=60])

Comprehensive Metabolic Panel	10 ppm Mean Change [95% CI: min, max] (*p* value)	32 ppm Mean Change [95% CI: min, max] (*p* value)	Total Sample Mean Change [95% CI: min, max] (*p* value)
Sodium [mmol/L]	-0.1[-0.7, 0.6] (0.87)	0.2 [-0.7, 1.0] (0.71)	0.03 [-0.5, 0.6] (0.90)
Potassium [mmol/L]	-0.1[-0.3, 0.02] (0.10)	-0.03 [-0.2, 0.1] (0.74)	-0.08 [-0.2, 0.03] (0.13)
Chloride [mmol/L]	-0.4[-1.2, 0.3] (0.23)	0.04[-1.1, 1.2] (0.94)	-0.3[-0.9, 0.4] (0.44)
Carbon Dioxide [mmol/L]	0.5[-0.5, 1.6] (0.33)	-0.04[-1.1, 1.0] (0.94)	0.3[-0.5, 1.1] (0.44)
BUN* [mg/dL]	-0.9[-1.7, -0.1] (0.03)**	0.5 [-1.1, 1.8] (0.41)	-0.3 [-1.1, 0.4] (0.37)
Creatinine [mg/dL]	0.01 [-0.02, 0.03] (0.60)	-0.02 [-0.04, 0.01] (0.21)	-0.003 [-0.02, 0.01] (0.74)
Glucose [mg/dL]	3.6 [-1.6, 8.7] (0.17)	-0.7 [-4.2, 2.9] (0.71)	1.9 [-1.5, 5.3] (0.28)
ALP [U/L]	-1.4 [-3.9, 1.1] (0.28)	2.0 [-1.0, 5.0] (0.18)	-0.03 [-2.0, 1.9] (0.97)
AST [U/L]	-0.44 [-2.1, 1.2] (0.60)	2.0 [-2.6, 6.5] (0.40)	0.5 [-2.0, 2.5] (0.61)
ALT [U/L]	-2.6 [-4.8, -0.3] (0.03)**	2.3 (-1.6, 6.3) (0.25)	-0.6 (-2.7, 1.5) (0.58)
Total Protein [g/dL]	-0.02 [-0.3, 0.2] (0.87)	0.2 [-0.001, 0.4] (0.051)	0.1 [-0.1, 0.3] (0.45)
Total Bilirubin [mg/dL]	-0.02 [-0.08, 0.3] (0.43)	-0.03 [-0.11, 0.05] (0.49)	-0.02 [-0.07, 0.02] (0.29)
Albumin [g/dL]	-0.07 [-0.1, 0.0004) (0.06)	0.11 [-0.01, 0.23] (0.09)	0.002 [-0.07, 0.07] (0.96)
Calcium [mg/dL]	-0.1 [-0.2, 0.04] (0.20)	0.1 [-0.003, 0.2] (0.06)	0.0 [-0.1, 0.1] (0.99)

*BUN- Blood Urea Nitrogen; ALP: Alkaline Phosphatase; AST: Aspartate Aminotransferase; ALT: Alanine Aminotransferase
**$p \leq 0.05$ Comparison of 10 ppm or 32 ppm active solution vs. placebo solution, controlling for baseline value, in a mixed effects linear regression model.

Table 4: Reactive Oxygen Species and Pro-inflammatory Cytokine Analyses

ROS or Cytokine Parameter	10 ppm Mean Change [95% CI: min, max] (*p* value)	32 ppm Mean Change [95% CI: min, max] (*p* value)	Total Sample Mean Change [95% CI: min, max] (*p* value)
ROS μM	0.89 [-0.6, 2.38] (0.24)	-0.44 [-1.23, 0.35] (0.28)	0.52 [-0.56, 1.60] (0.34)
IL-8 (copies/1000 B2M)*	2.19 [-1.53, 5.91] (0.25)	6.39 [-5.83, 18.60] (0.31)	4.52 [-2.47, 11.51] (0.21)
IL-1α (copies/1000 B2M)	-0.0005 [-0.0007, 0.0006] (0.88)	0.0197 [-0.0014, 0.0408] (0.07)	0.0128 [-0.0014, 0.0269] (0.08)
IL-1β (copies/1000 B2M)	0.017 [-0.011, 0.044] (0.24)	0.027 [-0.058, 0.112] (0.53)	0.022 [-0.027, 0.072] (0.38)
MCP1 (copies/1000 B2M)	-0.028 [-0.084, 0.028] (0.34)	-0.004 [-0.026, 0.017] (0.69)	-0.015 [-0.046, 0.015] (0.33)
NQO1 (copies/1000 B2M)	-0.0043 [-0.0115, 0.029] (0.24)	-0.0279 [-0.4671, 0.4114) (0.90)	-0.0182 [-0.2850, 0.2487] (0.89)

ROS: Reactive Oxygen Species; B2M: Beta-2 microglobulin; MCP1: Monocyte chemoattractant protein -1; NQO1: NADH quinine oxioreducatase-1

Figures

Figure #1: Complete Blood Count with Differential Panel

Panel A: Change in Erythrocyte Counts

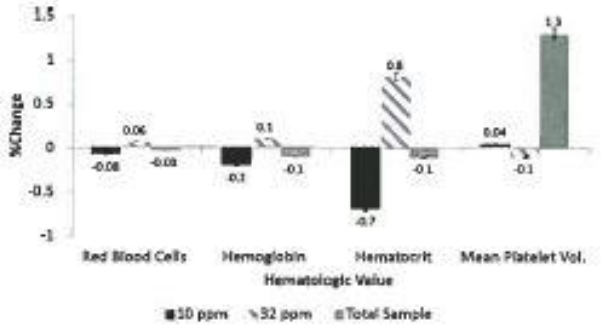

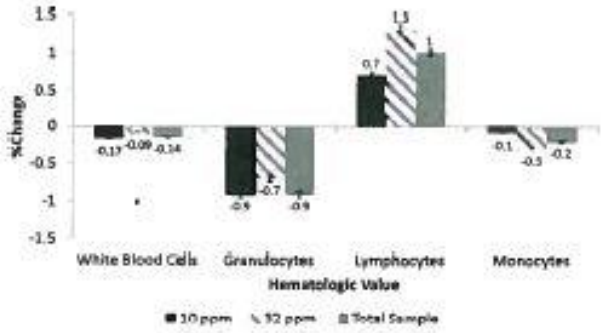

Panel B: Change in Granulocyte and Agranulocyte Counts